NANOSTRUCTURES IN COAL-DERIVED CARBONS

Robert Hurt, Joseph Calo, Ying Hu
Division of Engineering
Brown University
Providence, RI 02912

INTRODUCTION

Carbon nanostructure, the local spatial arrangement and orientation of graphene layers, affects many important properties of carbon materials, including mechanical strength and modulus [1,2], coefficient of thermal expansion [2], electrical properties [3] and their directional dependencies, pore size distribution [4,5], and reactivity to oxidizing gases [5]. In coal-derived carbons in particular, the nanostructure influences surface area and fine porosity of coal-derived sorbents, coke strength and gas reactivity, and the graphitizibility of anthracites. This paper examines the fundamental mechanisms that determine nanostructure in carbon materials, with special emphasis on coal as the organic precursor. In common with Professor Suuberg's studies of tar vapor pressures, this work involves the physical chemistry of pyrolysis and carbonization.

RESULTS AND DISCUSSION

Figure 1 shows two example nanostructures in flame-derived coal chars. Structure A exhibits long range orientational order with statistical fluctuations (meandering) about the mean orientational vector. This nanostructure is believed to arise through liquid crystal formation during the fluid stage of carbonization. Structure B exhibits only short range orientational order, in the form of recognizable "crystallites". In some carbons these crystallites are oriented completely at random, while in the lignite char sample in Fig. 1B there is some degree of preferential orientation among the crystallites. The following sections discuss the quantitative description of these structures and the mechanisms of their formation.

Quantification of order
HRTEM fringe images allow quantification of nanostructure by digital image analysis [6-8]. The results are best described as semiquantitative, due to the extremely small sample size probed by the electron beam and the difficulty obtaining statistically significant data for correlation to bulk sample properties. The order parameter, $S = 1/2 < 3 \cos\theta - 1 >$ is a measure of long-range anisotropy, where θ is the angle between a single layer (or line in 2D) and the mean orientational vector, and $<>$ denotes an average. If the anisotropy extends over supramicron length scales it can be easily detected by optical microscopy (where it is referred to as coke texture) and quantified as the difference between the minimum and maximum reflectance upon optical stage rotation under polarized light (optical bireflectance).

Determination of the long-range order parameter for the structures in Fig. 1 yields 0.9 for structure A and 0.6 for the structure B. An analysis based on liquid crystal theory has shown that the 0.9 order parameter is consistent with a liquid crystal formation mechanism, while 0.6 is not [8]. The low grade orientational order in the lignite sample is believed to be caused by strain induced alignment during carbonization [8].

Phase behavior of PAH mixtures
The formation of anisotropic carbon via the liquid crystal route can be treated as a problem in liquid / liquid phase equilibrium [9,10]. As molecular weight increases during carbonization, so does aspect ratio of the oligomers formed from the primary aromatic clusters. At a critical aspect ratio, the oligomers undergo a concerted alignment to form the ordered fluid, which upon further molecular weight growth undergoes a glass transition to form a solid carbon. In PAH mixtures, phase separation occurs in which the higher molecular weight components partition preferentially into the liquid crystalline phase, and lower molecular weight components into the isotropic phase. Further polymerization causes the mesophase (LC phase) to grow at the expense of the isotropic phase until one or both phases solidify.

The quantitative description of this phase behavior is complicated by the lack of model compound studies showing this behavior. Indeed, no pure polyaromatic hydrocarbon has ever been observed to form a discotic liquid crystal! A recent analysis suggests that this paradox is a mixture effect [10]. In complex multicomponent PAH mixtures, crystalline solid phases are suppressed and the underlying liquid crystalline phases are revealed. Figure 2 illustrates this effect in a hypothetical binary mixture. In multicomponent calculations, it is possible for a mixture of N nonmesogens to give rise to liquid crystalline phases due to the severe depression of the liquid / solid phases transition temperatures.

The latent liquid crystal forming tendency in PAH increases with increasing molecular weight (for similar structures), and in a complex mixture, the entire molecular weight distribution influences whether or not the liquid crystalline phase appears. Macroscopic

solution thermodynamics can be used to estimate the amount and compositions of the isotropic and anisotropic phases given the overall molecular weight distribution of the melt [10]. This solution thermodynamics approach is not valid in the low molecular weight limit — i.e. it does not give the correct results for solvents with no liquid crystal forming tendency (nonmesogens). Statistical models based on pseudo-potentials for orientation give a useful description of nonmesogen behavior [9], but are difficult to solve in the general multicomponent case involving N mesogens with differing molecular weights and clearing temperatures. More work is needed to develop comprehensive, tractable equilibrium models of mesophase formation.

Role of Fluidity

In low viscosity pitches, mesophase typically appears as Brooks-Taylor mesospheres, which are thermodynamically favored as they possess the minimum mesophase / isotropic interfacial area. The high viscosities in coal carbonization prevent this thermodynamic state from being reached and lead to irregularly-shaped anisotropic domains. Nonfusible material can also limit the growth and coalescence of mesophase by collecting at the boundaries between the mesophase and isotropic phases or between mesophase regions (domains) of different orientation.

At still lower mobility (higher viscosity), the primary formation of carbonaceous mesophase is suppressed, and the resulting carbon has very short range orientational order (5 - 10 nm). Figure 3 shows results of a numerical simulation that addresses the effect of layer mobility on liquid crystal phase transitions [11]. The simulations employ hard lines which rotate and grow in a two-dimensional continuum. At high mobility (rotational frequency) the lines adopt orientational order at a certain length to avoid overlap. At lower mobility, the lines form finite ordered regions in an isotropic matrix, thus mimicking the observed behavior of carbons. Figure 4 plots the order parameter as a function of the dimensionless mobility-to-growth ratio. The numerical model in its simplest form is sufficient to distinguish two important classes of carbon materials: (1) isotropic carbons formed via all-solid-state routes in which molecular mobility is severely limited (e.g. low-rank coals, woody and cellulosic materials, and oxygen-rich thermosetting polymers), and (2) anisotropic carbons formed from precursors that pass through a mobile, liquid-phase intermediate (high-rank bituminous coals, polyvinyl chloride, anthracene, many petroleum and coal-tar pitches).

It is further found that anthracitic order can be adequately represented by simulations in which the layers have a preferred initial direction (non-zero initial order parameter) and non-zero initial length (see Fig. 4). This is justified by TEM and NMR studies of raw anthracites which indicate that significant aromatic cluster development has occurred during coalification. The simulations in Fig. 4 show a gradual, monotonic increase in final order as the mobility increases, so that anthracites produce chars with long-range order intermediate between the high-rank bituminous coals and the low-rank materials. This simulation behavior is consistent with the observed rank trends.

Figure 5a,b show further comparisons between carbonization studies and the simple numerical simulations. Figure 5a shows measurements of optical bireflectance as a function of carbonization temperature for three coals of various rank [12]. These results are given as a function of temperature, rather than time, but are indicative of the solid structures observed during the various stages of carbonization, as they might occur during non-isothermal heat treatment. The lowest rank coal is isotropic it its initially state and remains essentially so during carbonization. The high-rank bituminous coal shows measurable anisotropy it its raw state, but loses this anisotropy at 400 °C, and regains it at slightly higher temperatures. Apparently the increase in mobility on heating allows the structure to relax from a metastable configuration imposed by high lithostatic pressure to a near equilibrium isotropic configuration at 1 bar pressure. As heating continues, molecular weight growth proceeds until the planar structures reach the critical size (aspect ratio) for liquid crystal formation, and a highly ordered state develops. The bireflectance thus passes through a minimum, as seen in Fig. 7 in the curve labeled high-rank bituminous. The anthracite in raw form shows significant anisotropy, which is unaltered up to 600 °C and then slightly enhanced by higher temperature heat treatment. Despite the high degree of initial order, the anthracite does not develop the same degree of order as the high-rank bituminous coal. This is consistent with the observation that many anthracites are nongraphitizable [13].

Finally, Fig. 5b shows time dependent simulation results for three cases representing important classes of coals. The simulations show that: (1) the low rank coal is nearly isotropic and remain so during carbonization, (2) the high rank bituminous coal loses its initial anisotropy, but regains it during the latter stages of carbonization, (3) the anthracite retains and slightly enhances its anisotropy during carbonization. Comparing Figs. 5a and 5b, it is seen that the simple hard-line simulations also mimic these major trends seen in the bireflectance studies. Overall, the concepts of liquid / liquid equilibrium, together with the kinetic effects associated with limited layer mobility can describe the formation of most carbon types. An exception, however, is isotropic coke, whose formation mechanism receives separate consideration in the next section.

Isotropic coke

Many coal chars pass through a fluid state, but solidify to form isotropic chars. The lack of long range order in these materials cannot be explained by low fluidity (high viscosity) — many of them exhibit higher maximum fluidities than coals which form anisotropic chars. A promising explanation for isotropic coke formation is the suppression of liquid crystalline phases by non-planar molecules, or "non-mesogens".

A key requirement for the formation of liquid crystalline phases is a high aspect ratio, L/D, of the rod-like or disk-like constituent molecules. Most functional groups that act as cross-linking agents for aromatic clusters (aryl, ether, sulfide) involve non-linear single bonds. These cross-links produce oligomers of aromatic clusters that can adopt both planar and nonplanar configurations upon bond rotation. Depending on the shape of the aromatic oligomer (influenced by the geometry of the aromatic clusters and side chains) the planar geometries may be stearically hindered, and the nonplanar structure that results may act as a "nonmesogen" and cause a local disruption in the liquid crystalline phase.

The effect of nonmesogens on LC phases has been studied in the canonical case of spherical solutes (L/D = 1) in rod-like mesogens [14]. Phase diagrams for binary mixtures of mesogens and nonmesogens have been derived from a statistical theory based on a pseudo-potential for orientation. Recently, Shishido [9] have applied this statistical theory to explain the suppression of mesophase in pitch by addition of low-molecular weight pitch fractions (which were presumed to be completely nonmesogenic).

Figure 6 presents a qualitative picture of this effect as it may occur during coal carbonization. Assuming a linear relationship between clearing temperature and molecular weight [10], the Bates-Shishido phase diagram can be plotted as MW vs. the mole fraction nonmesogen. The plot also shows two possible carbonization trajectories for a high-rank and low-rank bituminous coal. The trajectories were calculated using the measured elemental composition of the solid carbonizing phase, and assuming that a fixed fraction, F, of the oxygen and sulfur atoms were present as in functional groups that lead to non-planar cross-links. The average number of these non-planar groups per oligomer is:

$$N = F (X_{O+S}) (MW_{oligomer}) / (MW_{mixture})$$

where X_{O+S} is the mole fraction O and S atoms, and $MW_{mixture}$ is the mean atomic weight of the carbonizing melt. The mole fraction nonmesogens is then the probability that a given oligomer contains one or more non-planar links (and thus has an overall nonplanar geometry), which, assuming a Poisson distribution, is given by: $1 - \exp(-N)$.

Trajectories were drawn for various values of F in an attempt to reproduce the experimental fact that Illinois #6 flame chars are isotropic, while Pocahontas #3 chars are anisotropic (except for inertinite-derived material). A value of 0.05 gives reasonable behavior as shown in Fig. 6. Thus if only 5% of the O and S atoms are involved in nonplanar cross-linking structures, liquid crystal formation will be largely suppressed in the low-rank Illinois #6 coal. This is the most promising explanation for the overall trend of isotropic coke formation from many oxygen-rich and sulfur-rich precursors. The full quantitative relation between chemical functionality and mesogenicity is, of course, complex and must be based on functional group analysis rather than simple elemental analysis.

It is evident from this paper that much more work is needed before we have a complete quantitative understanding of the origin and evolution of carbon nanostructures.

REFERENCES

1. Emmerich, F.G. *Carbon* 33 47 (1995).
2. Sato S., Kawamata, K., Kurumuda, A., Kawamota, M., Ishida, R. *Carbon* 26 (4) 465 (1988).
3. Rouzaud, J.N., Oberlin, A. *Carbon* 27 (4) 517 (1989).
4. Oberlin, A., in *Chemistry and Physics of Carbon, Vol. 22*, ed. P. A. Thrower, Marcel Dekker, New York, 1989, pp. 1-143.
5. Rouzaud, J.N., Oberlin, A. Chapt. 17 in *Advanced Methodologies in Coal Characterization*, Elsevier, Amsterdam, 1990.
6. Palotas, A. B., Rainey, L. C., Feldermann, C. J., Sarofim, A. F., and Vander Sande, J. B., *Microsc. Res. Tech.*, 1996, 33, pp. 266-278.
7. Dobb, M. G., Guo, H., and Jonhson, D. J., *Carbon*, 33 1115 (1995).
8. Shim, H.S., Hurt, R.H., Yang, N.Y.C. "A Methodology for Analysis of 002 LF Fringe Images and Its Application to Combustion-Derived Carbons", *Carbon*, in press.
9. Shishido, M., Inomata, H., Arai, K, Saito, S. *Carbon* 35 (6) 797 (1997).
10. Hurt, R.H., Hu, Y. "Thermodynamics of Carbonaceous Mesophase," *Carbon*, in press, 1998.
11. Hu, Y., Calo, J.M., Hurt, R.H., Kerstein, A. "Kinetics of Orientational Order / Disorder Transitions and Their Application to Carbon Material Synthesis," *Modelling and Simultion in Materials Science and Engineering*, in press.
12. Murchison, D.G., Chap. 31 in *Analytical Methods for Coal and Coal Products*, Academic Press, New York, 1978.
13. Blanche, C., Dumas, D., Rouzaud, J.N. Coal Science (Pajares and Tascon Eds.) Elsevier Science, Amsterdam, 1995, p. 43.
14. Humphries, R.L., and Luckhurst, G.R. *Proc. R. Soc. London, A.* 352 41-56 (1976).
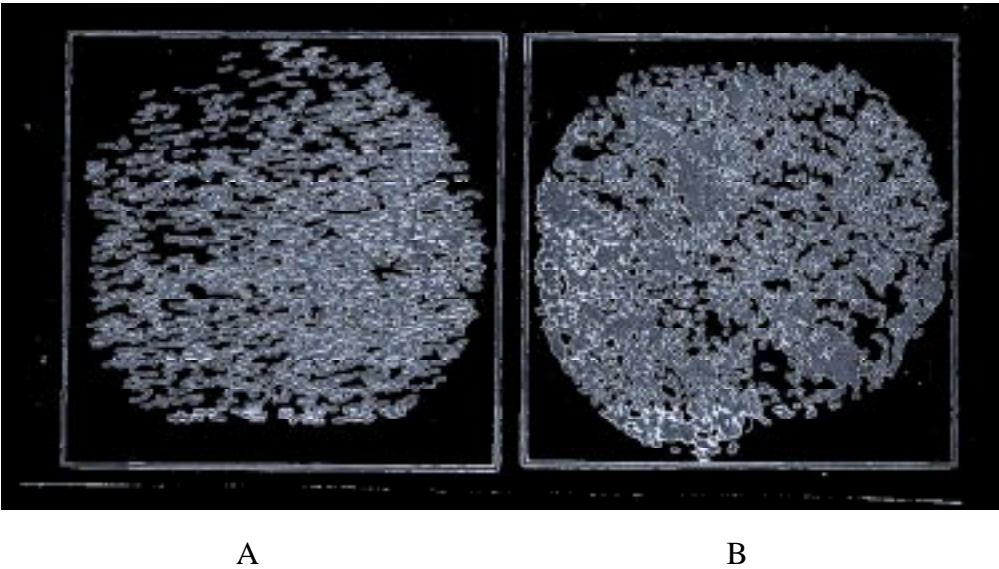
A   B

Figure 1. Digitally enhanced high resolution TEM fringe images showing the nanostructures of coal-derived carbons. The lines are graphene layers, imperfect snippets of the graphite lattice, viewed edge-on. A: Pocahontas #3 char; B: lignite char.
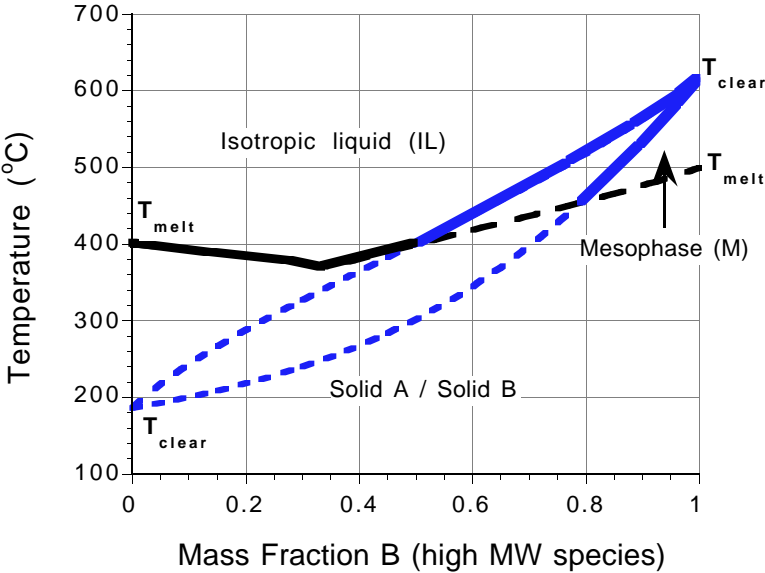

Figure 2. Example binary phase diagram for generic PAH of low and high molecular weight.   In the pure state A is nonmesogenic and B is mesogenic.
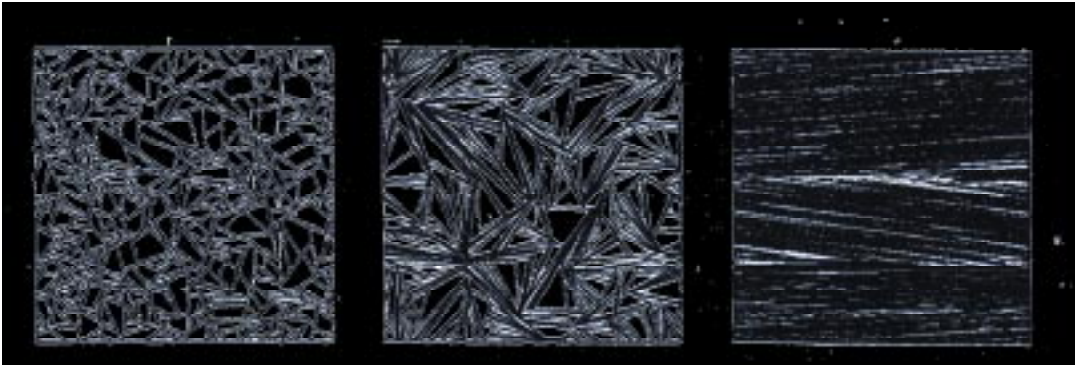

Figure 3. Summary of frozen states in hard-line simulations. As mobility/growth ratio, M*, increases, the final structures changes from complete disorder to short range order to a structure in which the ordered length scale is comparable to the size of the simulation box.

Figure 4 Summary of final states in numerical simulations starting from initially random states (isotropic parent materials) and initial ordered states (anisotropic parent materials). Long-range order parameter in the final state vs. dimensionless mobility / growth ratio, $M*$. Curve labels show the relation to carbonization processes. Type A carbons: isotropic solids formed through solid-state pyrolysis (e.g from lignites, woody tissue, oxygen-rich polymers); Type B carbons: anisotropic solids formed through liquid phase pyrolysis (pitches, polyaromatic compounds, coking coals); Type C carbons: anisotropic solids formed by solid-state pyrolysis of initially ordered precursors (e.g. anthracites).
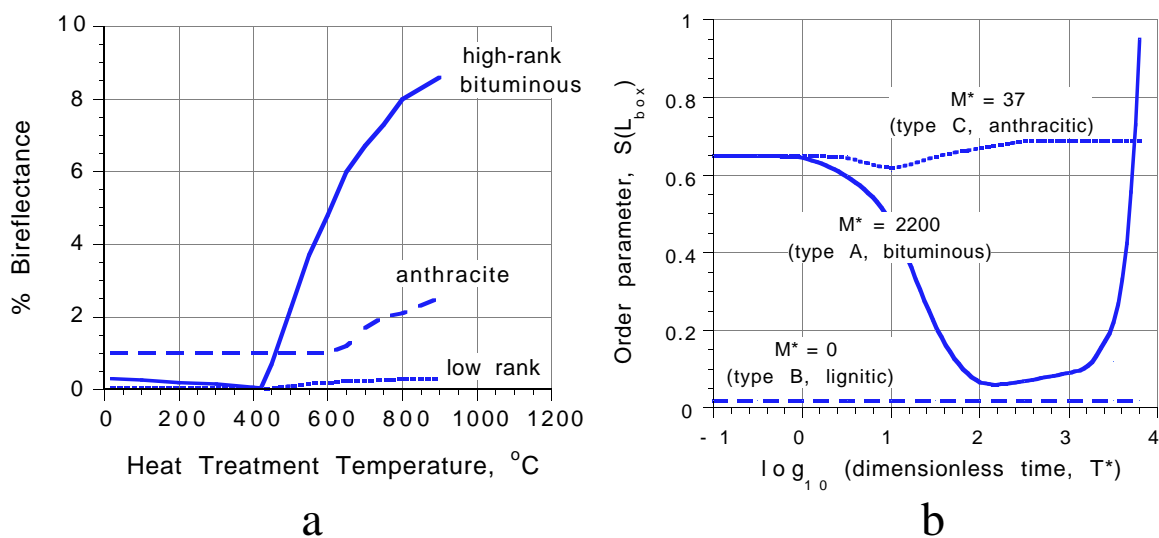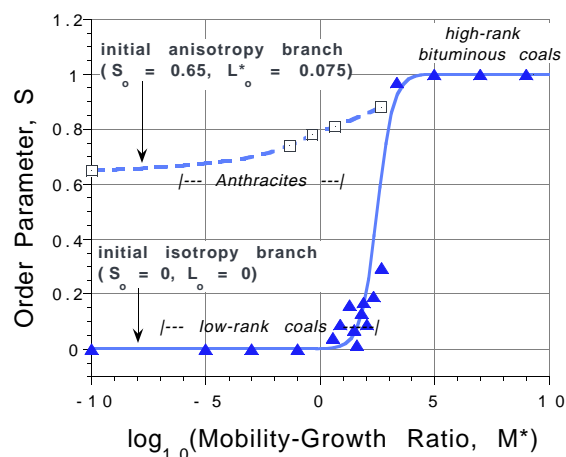
Figure 5. a: Measurements of optical bireflectance as a function of carbonization temperature for three important classes of coals from Murchison [12]; b: Time evolution of the long-range nematic order parameter in three simulations representing important classes of carbonization processes.
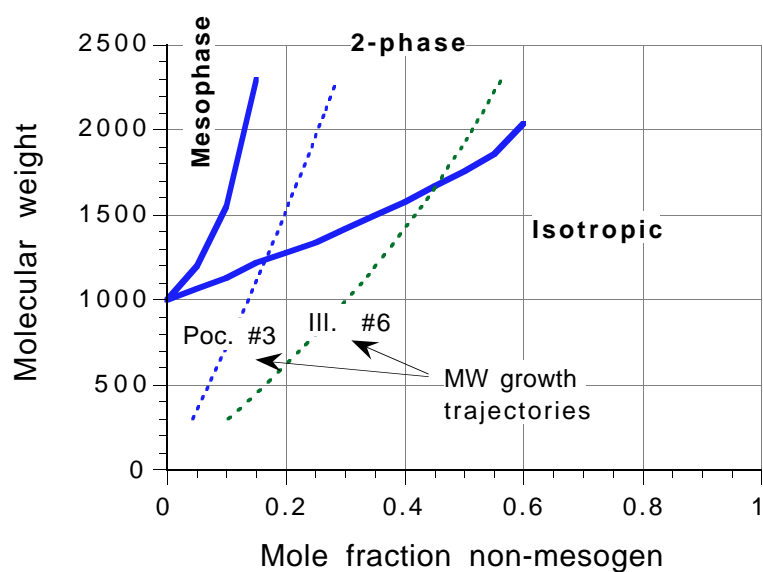
Figure 6 Phase diagram for binary mixture of mesogens and nonmesogens showing possible trajectories describing the carbonization of bituminous coals of different rank. Plot is useful for developing a theory of isotropic coke formation.